

## Taguchi Grey Relational Analysis of Mechanical Properties of Structural Steel Welding Made by Gas Tungsten Arc Welding

Saleh Suliman Saleh Elfallah <sup>1\*</sup>

*1 College of Mechanical Engineering Technology - Benghazi.*

Received: 22 / 03 / 2024; Accepted: 12 / 05 / 2024

### ABSTRACT

Welding is a widely used method in industry for joining metals. Its applications include structures, fabrications, automobiles, oil and gas production, and others. Gas Tungsten Arc Welding (GTAW) is a common welding technique that produces higher-quality welds. Its application is mostly for stainless steel and aluminum welding due to its stable arc and focused heat source that produces a narrower heat-affected zone (HAZ). However, optimizing the welding process is a challenge for better-quality welds. This study utilizes the Grey-Taguchi method to optimize welding parameters for maximum tensile strength and hardness of structural steel welds. Structural steel, one of the most common materials involved in local industry, is normally welded by shielded metal arc welding (SMAW), while this work inspects the mechanical and microstructure properties of welds made by GTAW. The results presented higher tensile strength of weldments with decreased welding current. The V-groove-shaped weldments' tensile strength was higher than that of the samples with X-groove-shaped weldments. The Taguchi method has obtained that welding tensile strength is mostly influenced by the welding current, followed by groove shape, while welding speed has the least impact on the tensile strength. The grey relational analysis (GRA) concluded that groove shape had a higher impact on multi-response analysis. The welding factor's optimum settings are 170 A, groove shape V, and a welding speed of 150 mm/min.

**KEYWORDS:** Structural steel, GTAW, Tensile strength, Hardness, Grey-Taguchi method.

### 1. INTRODUCTION

Welding is considered one of the most common manufacturing techniques in the industry for joining metallic alloys. It's simple, flexible, and produces high-strength joints. Gas tungsten arc welding (GTAW) is a known welding process used mostly to weld aluminum, stainless steel, and dissimilar alloys. Furthermore, it uses non-consumable tungsten as an electrode. Moreover, GTAW is advantageous for producing high-quality welds with focused heat generated between the electrode and the welding joint, which produces minimum distortion welds with maximum penetration. In addition, GTAW is fumeless, spatter-free, and normally requires no finishing process. Besides, it's affordable. <sup>[1,2,3]</sup>

Carbon steel is extensively utilized in various engineering applications, such as structures, gears, vices, cutting tools, shafts, railways in fabrication, and others. Each application selects the suitable carbon steel based on properties that are determined principally by the alloy's carbon content. Structural steel, or low-alloy steel, is widely involved in fabrication in local industry.

It is shaped by various fusion welding techniques such as shielded metal arc welding (SMAW), gas metal arc welding (GMAW), and gas tungsten arc welding (GTAW). Also, non-fusion techniques such as friction stir welding (FSW). <sup>[4,5]</sup>

The issue with weldments in general is that the differences in mechanical characteristics between the base metal, the fusion zone (FZ), and the heat-affected zone (HAZ) can lead to failure. This is a result of the variations in grain size and structure among them. <sup>[4,6]</sup> Weldment needs to have higher mechanical qualities, such as tensile strength and hardness, in order to prevent microscopic flaws and eventual failure. <sup>[7]</sup> Therefore, for high-quality weldments with improved mechanical properties, it's critical to optimize the welding parameters that govern the characteristics of the final weldment. <sup>[8]</sup> The tensile test is a well-known mechanical test that examines how much a material can extend before breaking, and in the case of testing welds, it is considered a common test. The hardness of materials or welds normally correlates linearly with their tensile strength. <sup>[9,10]</sup>

Various researchers studied the effect of GTAW welding parameters such as welding current, welding speed, filler material and diameter, root gap, gas flow rate, and others on the final weldment characteristics of

\*Correspondence: Saleh Suliman Saleh Elfallah

[sselfallah87@gmail.com](mailto:sselfallah87@gmail.com)

steel and other metal alloys. [2,11] For instance, Korkmaz et al. studied the effect of welding current and welding speed tensile strength on the welding of XPF800 steel by GTAW and 99.9% argon (Ar) as shield gas. The results found that higher tensile strength (777 MPa) was shown at 140 A and 100 mm/min [12]. The Taguchi method is a technique that is common in process optimization in industry [13]. It promotes the orthogonal array (OA) as a process design that requires fewer experiments than other design of experiment (DoE) methods [14]. Researchers have repeatedly utilized the Taguchi method to optimize GTAW weldment responses [15]. Numerous studies have experienced Taguchi's design to optimize the steel welding parameters made by GTAW on mechanical properties such as tensile strength and hardness. A study by Yadav et al. focused on dissimilar welding of AA5083 and AA6082 aluminum alloys and ER4043 as welding fillers. The work experimentation followed L9 OA and concluded that welding speed had a higher effect on the tensile strength and Brinell hardness, followed by welding current, while filler diameter had the least significant influence on the responses [11]. Mohanty et al. reported on low-carbon steel welding using welding filler grade ER309L and pure Ar as a shielding gas. The experiments designed according to L9 Taguchi's orthogonal array showed that welding current had a higher effect on welding tensile strength and hardness. The results revealed that the hardness was more affected by the welding speed, whereas the tensile strength was more affected by the welding voltage and current. Furthermore, a drop in welding voltage and current and an increase in welding speed were associated with an increase in tensile strength. Moreover, the FZ hardness varied as the welding tensile strength increased; at a maximum tensile strength of 473 MPa, the hardness was 147.2 HB, but at a maximum welding hardness of 151.2 HB, the tensile strength was 462.8 MPa [1]. Abima et al. reported on the welding of AISI 1008 low-carbon steel by welding filler ER70S-6 and found that lower welding current (140 A) and gas flow rate (15 L/mm) showed higher hardness (189.22 HV for FZ and 152.5 HV for HAZ). Furthermore, an increased tensile strength (432.89 MPa) was obtained at a higher welding current of 180 A and a gas flow rate of 19 L/mm [16]. Additionally, Jawad et al. reported on welding AISI 1045 medium steel that a maximum tensile strength of 625 MPa and Rockwell hardness of 80.19 HRB achieved at optimum welding speed, welding current, and gas flow rate. The study further concluded that increased tensile strength was detected at decreased welding speeds [17]. These studies and others infer that common welding parameters influence the tensile strength and hardness of weldments; however, the results show a change in the influence of parameters from one study to another. Nevertheless, according to the literature, the welding current had mostly higher control over the final weldment properties.

This work aims to optimize the GTAW welding process to produce reliable and quality S235JR structural steel weldments. GTAW is not familiar with welding structural steel; however, more research is needed to investigate the potential for GTAW to enhance structural steel weldments and increasingly emerge in the industry along with common techniques such as SMAW and GMAW in steel welding. The parameters that could have higher order effects have been included in addition to the groove shape, as it has not been commonly reported, as well as the welding current and welding speed as welding parameters. The objective of this study is to improve the tensile strength and hardness for quality and reliable weldment. The influence of each response was determined by the Taguchi method, while the effect of tensile strength and hardness was computed by the Grey Relational Analysis (GRA) method in multi-response optimization. In addition, the impact weights of the parameters on the objective functions were computed with the aid of the analysis of variance (ANOVA) approach.

## 2. MATERIALS AND METHODS

The structural steel also called low-alloy steel grade S235JR follows European Steel and Alloy (1.0038) is common in the local market in plate form. The plate that is 10 mm in thickness was cut by a computer numerical control (CNC) laser cutter in the Tasamim workshop at Benghazi to 50 mm by 450 mm. These rectangular shapes will bear the tensile strength and hardness samples after the welding process. The tensile strength samples followed the American Society of Testing Materials (ASTM) E8 / E8M [18] as shown in Figure 1. The grooves took V and X-like shapes with 60° for each angle (Figure 1). After the welding process, the rectangular parts were shaped into tensile samples by cutting through the reduced section (Figure 1), and those excess parts were taken to test the hardness of weldments. The welding of the samples has taken place at Altaibat Food Inc. The welded samples (weldments) are seen in Figure 2. The welding was processed using a power supply GTAW with tungsten as an electrode, a Daewoo Inverter Welder, tungsten inert gas / manual metal arc welding TIG/MMA, and a welding speed device that controls the electrode, the YSG-12 Beetle Portable Gas Cutter. The shielding gas for welding used is composed of 90% Ar and 10% carbon dioxide (CO<sub>2</sub>) with a flow rate of 10 L/min. Normally, a binary gas mixture of 80% Ar and 20% CO<sub>2</sub> is common in the welding of structural steel in the local industry, and 95% Ar and 5% CO<sub>2</sub> in other countries as shielding gas. The Ar protects the weld pool from atmospheric oxidation while the CO<sub>2</sub> promotes penetration depth in steel welding although in cases sputtering [19] (Mariappan et al., 2021). However, a study by Murali et al. showed slightly decreased tensile strength for alloy steel welded using 80% Ar and 20% CO<sub>2</sub>

mixture gas compared to pure Ar [20]. The welding filler utilized for welding is mild steel E6013 with a size of 2.5 mm. Table 1 lists the composition of the base metal and filler wire. Table 2 obtain the tensile strength and hardness properties of the structural steel or base metal and welding filler.

The parameters that vary in GTAW are welding current (A), welding speed (B), and groove shape (C) as mentioned earlier each has two levels, as listed in Table 3. The voltage is estimated to be between 20 V and 30 V. The welding experiments follow the 2-level's three parameters, resulting in a total of 8 runs as seen in codes in Table 4. This method is known as Taguchi's L8 array. Table 5 lists the experiments with the results, the tensile strength, and hardness values. The analysis was computed by Minitab 18®.

The tensile test was performed on the universal testing machine Shimadzu (UEH-20) at the Libyan Iron and Steel Company. The samples following the test are shown in Figure 3 presenting fractures in the welding area. The samples that failed quickly were repeated to guarantee the consistency of the results. The hardness test was carried out by Ernst Rockwell with a pressure force of 100 kg (HRB) and ball indenter sized 1/16 at the College of Mechanical and Engineering Technology. The tensile strength and Rockwell hardness HRB are presented in Table 5.

The heat input generated by welding as presented in Table 5 was calculated from Equation 1:

$$H = \frac{f_1 \times E \times I}{v} \quad (1)$$

Where  $f_1$  is the heat transfer factor or efficiency (0.6),  $E$  is the voltage (V),  $I$  is the current (A), and  $v$  is the travel speed (mm/s). The voltage was considered 30 V knowing that voltage of the welder machine reduces with working time due to the decreased efficiency.

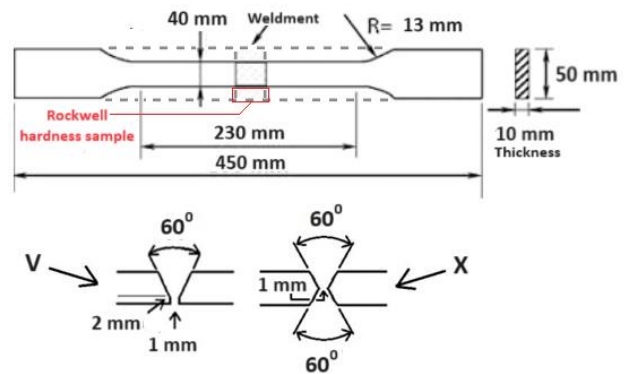


Fig.1. Samples dimensions for tensile test made according to ASTM E8/E8M [18]

Table 1. The chemical compositions of the base metal and welding filler used in the experiment [21]

Component	Composition									
	C	Mn	S	Ni	Cr	P	Si	Cu	Mo	V
Base metal (S235JR)	0.17%	1.4%	0.025%	0.012%	-	0.025%	-	0.55%	-	-
Welding filler (E6013)	0.10%	0.6%	0.03%	0.3%	0.2%	0.035%	0.5%	0.35%	0.2%	0.05%



Fig.2. Weldments

**Table 2. The tensile strength and hardness of base metal and welding filler** <sup>[22,23,24]</sup>

Component	Tensile properties		Hardness properties	
	Yield strength	Tensile strength	Elongation	Rockwell hardness B
Base metal (EN 10025-2)	235	360-510	26%	66.7 HRB
Filler wire (E6013)	458MPa (66.5ksi)	527MPa (76.5ksi)	25%	83 HRB

**Table 3. Parameters of the welding process each has two levels**

Code	Parameters	Unit	Level 1	Level 2
A	Welding current	A	170	200
B	Welding speed	mm/min	100	150
C	Groove shape	-	V	X

**Table 4. The orthogonal array layout L8 (2<sup>3</sup>) in a coded layout**

Trial	A	B	C
1	1	1	1
2	1	1	2
3	1	2	1
4	1	2	2
5	2	1	1
6	2	1	2
7	2	2	1
8	2	2	2

**Table 5. The experiments L8 and their corresponding responses (Tensile strength and hardness)**

Trial	Welding current (A)	Welding speed (mm/min)	Groove shape	Tensile strength (N/mm <sup>2</sup> )	Heat input (J/mm)	Hardness (HRB)	EL %
1	170	100	V	232	1836	82.5	4
2	170	100	X	202	1836	80.7	3
3	170	150	V	219	1224	84.8	4
4	170	150	X	191	1224	83.5	3
5	200	100	V	184	2160	83.8	3
6	200	100	X	158	2160	81.6	3
7	200	150	V	205	1440	80.4	4
8	200	150	X	169	1440	78.1	3



Fig.3. Weldments after tensile test showing fracture in the welds (FZ and HAZ)

### 3. RESULTS AND DISCUSSION

#### a. Effect of Welding Parameters on the Mechanical Properties

Table 5 illustrates how tensile strength has frequently increased with decreasing hardness and vice versa. For instance, the welding hardness increased from 82.5 HRB to 84.8 HRB at 170 A due to the lowered tensile strength from 232 to 219 N/mm<sup>2</sup> at V-groove-shaped weldments-shaped welding samples or trials. The enhanced tensile strength from 158 to 169 N/mm<sup>2</sup> at X-groove-shaped weldments-shaped welding samples, however, revealed a drop in welding hardness from 81.6 HRB to 78.1 HRB at 200 A. With an increase in welding speed, there has also been variation in the tensile strength. Overall, the increase in welding current from 170 A to 200 A and the rise in average heat input, which is influenced by welding speed and welding current, have resulted in a loss in tensile strength and hardness. In addition, it was greater at welding samples with V-groove-shaped weldment shapes. The sample elongated to 4% increase in length at a tensile strength of 232 N/mm<sup>2</sup>, compared to 3% at 158 N/mm<sup>2</sup>, indicating that the elongation was higher at the increased tensile strength.

Table 5 illustrates how increased welding current with decreased welding speed led to increased welding heat input. Equation 1 is used to compute the welding heat input. For instance, in trials 1 and 5 in Table 5, the welding current rose from 170 to 200 A, resulting in an increase in the heat input from 1836 to 2160 J/mm. Additionally, the heat input has dropped from 1836 to 1224 J/mm due to the higher welding speed of 100 to 150 mm/min.

Increased internal tensions resulting from the fusion zone's greater dilution caused by the welding's prolonged heat [25]. Lower weldment tensile strength and hardness in

the welding looked to be a result of the greater internal stresses. Table 5 makes it evident that increased heat input was observed at increased welding amperage, which is correlated with decreased hardness and tensile strength. The Taguchi method study will include a presentation of the increased influence of welding current later on. The samples with lower weldment tensile strength are the ones that were manufactured at an X-groove shaped weldments shape and the samples made at a V-groove shaped weldments shape at a higher welding current (200 A), as shown in Figure 3 for samples (trials) 2, 4, 5, 6, 7, and 8. A longer cooling rate is a result of the increased heat input from a microstructural standpoint. As a result, the welding area has coarser grains due to a longer microstructural recrystallization time [26]. In a previous similar study made on structural steel welded by GTAW, it was found that faster welding speeds led to reduced heat input, coarser  $\alpha$ -ferrite grain formation, and less carbide and Widmanstatten ferrite in the welding area. Higher weldment tensile strengths in welding have resulted from it [27]. While lower heat input due to lower welding current has caused the formation of finer  $\alpha$ -ferrite and increased precipitation of Widman Tatten ferrite, a study by Abima et al. on low-carbon steel welding metallurgy agrees that lower heat input has increased welding weldment tensile strength and HAZ hardness [16]. The data do not clearly show that increased weldment tensile strength is a function of increased welding hardness. As was previously mentioned, the welding tensile strength has been demonstrated to be influenced by the groove shape, and the dilution is the outcome of the welding heat input caused by the welding current. As Table 2 illustrates, the tensile strength of welding has generally been demonstrated to be lower than the tensile strength of base metal and welding filler. As Table 2 illustrates, the hardness of the welding was comparable to that of the welding filler. Stated

differently, the weldment tensile strength of the welding was unaffected by the hardness differential between the welding area and the nearby base metal. The failure at the edge of the welding region due to the softening of HAZ is believed to be caused by increased heat input, which led to increased strains in the welding area, even if the dilution wasn't higher for the experiments that were exposed to lower heat input. It was stated that HAZ has larger residual stresses than the welding area [28], and its softening is the cause of the hardness loss [29].

**b. Taguchi Method**

The primary impacts of signal-to-noise (S/N) ratios for tensile strength and hardness are presented in Table 6, while the plot for mean S/N ratio for tensile strength and hardness are shown in Figures 4 and 5, respectively. S/N ratio demonstrates the impact of the welding settings measuring the noise level under various noise situations for the response.

**Table 6. S/N ratios correspond to the tensile strength and hardness values**

Trial	Welding current (A)	Welding speed (mm/min)	Groove shape	Tensile strength S/N ratio	Hardness S/N ratio
1	170	100	V	47.3098	38.3291
2	170	100	X	46.1070	38.1375
3	170	150	V	46.8089	38.5679
4	170	150	X	45.6207	38.4337
5	200	100	V	45.2964	38.4649
6	200	100	X	43.9731	38.2338
7	200	150	V	46.2351	38.1051
8	200	150	X	44.5577	37.8530

The experiment goal, which is to maximize the responses as indicated by equation 2, is correlated with the greater S/N ratio, which is designated as "Larger is Better".

$$\frac{S}{N} = -10 \log\left[\frac{1}{n} \sum_{i=1}^n \frac{1}{y_i^2}\right] \quad (2)$$

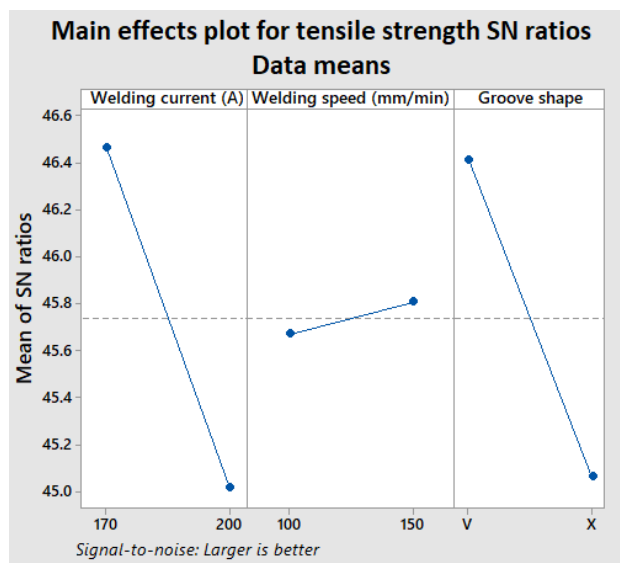


**Fig.4. Main effect plot of S/N ratios for weldments tensile strength**

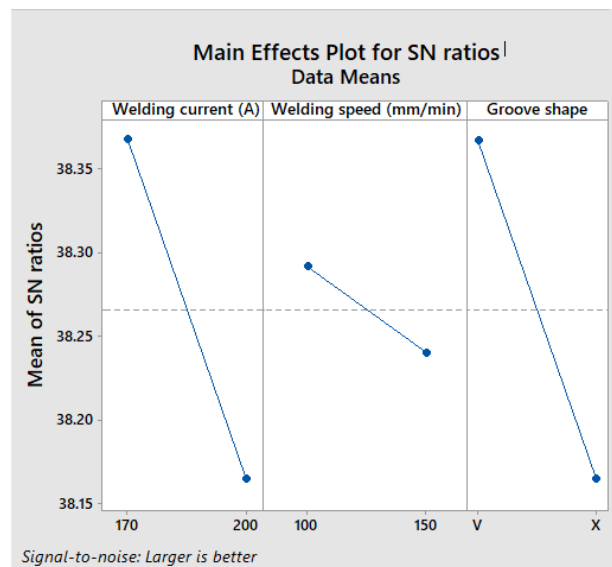


**Fig.5. Main effect plot of S/N ratios for weldments hardness**

The means of S/N ratios that are presented in Figure 4 and Figure 5 are listed in Table 7 and Table 8 respectively. The ranking in Table 7 and Table 8 are based on the higher delta value, which is the result of the S/N ratio of level 1 minus the value of level 2. The ranking presents the relative strength of each factor. As shown in Table 7, a welding current of 170 A has a greater S/N ratio (46.46) than a welding current of 200 A

(45.02). Comes second to the V-groove shaped weldments-shaped welding demonstrated a higher S/N ratio (46.41), compared to the X-groove shaped weldments-shaped welding, which demonstrated a 45.06 noise ratio. These values correspond to level 1 and level 2, respectively. As indicated by 150 mm/min, the welding speed had the least impact on the increased tensile strength, with a noise ratio of 45.67. The welding current 170 A and groove shape V both had the same ranking, thus similar impact on the weldment hardness. The welding current was ranked first in Table 7 and Table 8, which indicates it has higher influence or impact on the tensile strength and hardness of weldments.

The ANOVA in Table 9 and Table 10 confirm Taguchi's showing the higher contribution of welding current by 19.32 % and 1.59 % on the effect of the tensile strength and hardness respectively. The contribution values are listed as F in the tables. However, the P-value (population value) for the welding parameter has shown non-significant on the weldment hardness (Table 10) since the level of significance taken is 0.05. While the welding current and groove shape have shown a significance impact on the tensile strength (0.012 and 0.015 respectively) as presented in Table 9.

**Table 7. Ranking for means of S/N ratios for weldments tensile strength**

Level	Welding current (A)	Welding speed (mm/min)	Groove shape
1	46.46	45.67	46.41
2	45.02	45.81	45.06
Delta	1.45	0.13	1.35
Rank	1	3	2

\*Larger is better

**Table 8. Ranking for means of S/N ratios for weldments hardness**

Level	Welding current (A)	Welding speed (mm/min)	Groove shape
1	38.37	38.29	38.37
2	38.16	38.24	38.16
Delta	0.20	0.05	0.20
Rank	1	3	2

\*Larger is better

**Table 9. ANOVA for tensile strength S/N ratios**

Source	DF	Seq SS	Adj SS	Adj MS	F	P
Welding current (A)	1	4.18187	4.18187	4.18187	19.32	0.012
Welding speed (mm/min)	1	0.03592	0.03592	0.03592	0.17	0.705
Groove shape	1	3.63354	3.63354	3.63354	16.79	0.015
Residual Error	4	0.86572	0.86572	0.21643		
Total	7	8.71705				

**Table 10. ANOVA for hardness S/N ratios**

Source	DF	Seq SS	Adj SS	Adj MS	F	P
Welding current (A)	1	0.082290	0.082290	0.082290	1.59	0.276
Welding speed (mm/min)	1	0.005276	0.005276	0.005276	0.10	0.766
Groove shape	1	0.081805	0.081805	0.081805	1.58	0.277
Residual Error	4	0.207438	0.207438	0.051859		
Total	7	0.376809				

**c. Grey relational analysis (GRA)**

GRA is a technique developed to solve multi-objective or multi-response optimization. In order to obtain optimum tensile strength and hardness of weldments<sup>30</sup>. First, normalization was made on the response results by Equation 3 and shown in Table 11.

$$Y_i^*(k) = \frac{y_i(k) - \min(y_i(k))}{\max(y_i(k)) - \min(y_i(k))} \quad (3)$$

Where  $i = 1, \dots, m$ ;  $k = 1, 2, \dots, n$ ;  $m$  is the number of experimental data,  $n$  is the number of factors,  $y_i(k)$  = original sequence,  $Y_i^*(k)$  = value after grey relational generation (GRG),  $\min y_i(k)$  is the minimum value of  $y_i(k)$  and  $\max y_i(k)$  is its maximum value. The grey relational coefficient (GRC) is computed by Equation 4 and the coefficients are shown in Table 12.

$$\varepsilon_j(k) = \frac{\Delta_{\min} + \omega \Delta_{\max}}{\Delta_{oi}(k) + \omega \Delta_{\max}} \quad (4)$$

Where,  $\Delta_{oi}$  is the deviation among  $Y_0^*(k)$  and  $Y_i^*(k)$ ,  $Y_0^*(k)$  is the ideal reference sequence,  $\Delta_{\min}$  is the least value of  $\Delta_{oi}(k)$  and  $\Delta_{\max}$  is the highest value of  $\Delta_{oi}(k)$ . Table 4 gives the calculated Grey relation coefficients. The grey rational grade (GRG) is calculated by Equation 5 and shown in Table 12.

$$\Gamma_i = \frac{1}{n} \sum_1^Q i(k) \quad (5)$$

Where,  $Q$  = total quantity of responses  $n$  is the number of output responses, while  $i$  is the level of the relationship between the reference and the comparative sequence. The means plot S/N ratio for GRG is shown in Figure 6, while Table 13 shows the ranking based on the S/N means and Table 14 presents the ANOVA.

**Table 11. Normalization of tensile strength and hardness results**

Trial	Welding current (A)	Welding speed (mm/min)	Groove shape	Tensile strength (Normalized)	Hardness (Normalized)
1	170	100	V	1.000	0.666
2	170	100	X	0.640	0.398
3	170	150	V	0.060	0.019
4	170	150	X	0.494	0.812
5	200	100	V	0.397	0.856
6	200	100	X	0.000	0.010
7	200	150	V	0.678	0.353
8	200	150	X	0.175	0.000

**Table 12. GRC and GRG for the tensile strength and Hardness**

Trial	Welding current (A)	Welding speed (mm/min)	Groove shape	Tensile strength GRC	Hardness GRC	GRG	S/N
1	170	100	V	1.429471	1.4742	1.451836	3.23835
2	170	100	X	0.495935	0.494022	0.494978	-6.10828
3	170	150	V	1.401621	1.449979	1.4258	3.08117
4	170	150	X	1.414338	1.479786	1.447062	3.20974
5	200	100	V	1.411469	1.481461	1.446465	3.20616
6	200	100	X	1.399882	1.44966	1.424771	3.07490
7	200	150	V	1.419805	1.462378	1.441092	3.17383
8	200	150	X	1.404977	1.449297	1.427137	3.08931

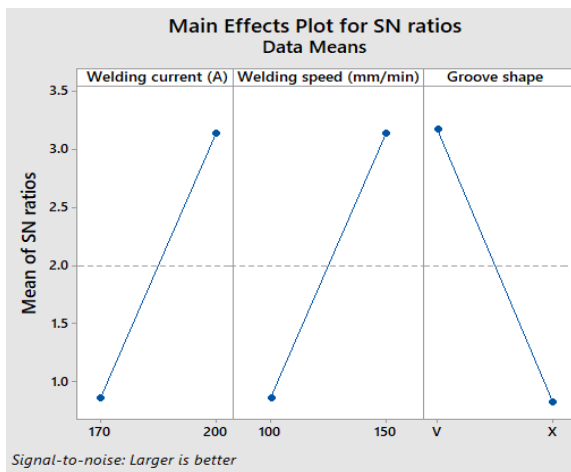


Fig.6. Main effect plot of S/N ratios for GRG

Table 13. Ranking for means of S/N ratios for GRG

Level	Welding current (A)	Welding speed (mm/min)	Groove shape
1	0.8552	0.8528	3.1749
2	3.1361	3.1385	0.8164
Delta	2.2808	2.2857	2.3585
Rank	3	2	1

Table 14. ANOVA for GRG S/N ratios

Source	DF	Seq SS	Adj SS	Adj MS	F	P
Welding current (A)	1	10.40	10.40	10.40	0.97	0.381
Welding speed (mm/min)	1	10.45	10.45	10.45	0.97	0.381
Groove shape	1	11.12	11.12	11.12	1.03	0.367
Residual Error	4	43.11	43.11	10.78		
Total	7	75.08				

The S/N ratio with optimal conditions is predictable by Equation 6:

$$\eta_{opt} = \eta_m + \sum_{i=1}^f (\bar{\eta}_i - \eta_m) \quad (6)$$

Where  $\eta_m$  = the mean of S/N ratio means,  $f$  = the number of parameters,  $\eta_i$  = the mean of the signal-to-noise ratios at the optimal level of each factor  $i$ .

Table 13 shows that groove shape has shown a higher rank which indicates it has a higher impact on the tensile strength and hardness and it showed a higher contribution on the response influence according to the F value in Table 14. However, none of the welding parameters has presented significance on both the tensile strength and hardness based on ANOVA.

It is evident from Taguchi method that the welding speed has the least impact on the weldment's tensile strength and weldment hardness, while the welding current, has demonstrated a stronger influence. The GRA showed based on multi-response analysis that groove shape showed a higher impact on the responses. The optimal welding conditions according to GRA are 170 A, V-shaped welding, and 150 mm/min.

#### 4. CONCLUSIONS

Structural steel was welded using GTAW with various welding settings. The effects of a combination of welding current, welding speed, and groove form on the hardness and weldment welding tensile strength were investigated. The Taguchi method is applied to the analysis. The outcomes showed that reduced welding current led to higher welded tensile strength. The tensile strength of the welding samples with a V-groove-shaped weldments was higher than that of the samples with an X-groove-shaped weldments. According to Taguchi, the welding tensile strength is mostly influenced by the welding current, with the groove shape having a somewhat similar effect. The welding speed has the least impact on the tensile strength. Furthermore, the GRA showed that groove shape had a higher effect on multi-response analysis. The welding factor's optimum combination is 170 A, groove shape V, and a welding speed of 150 mm/min.

#### 5. ACKNOWLEDGMENT

The author would like to thank his family for their support and encouragement throughout this study. A sincere appreciation goes to the Libyan Iron and Steel

Company for their help, to the staff of the welding laboratory at Altaibat Food Inc. An appreciation goes to the College of Mechanical Engineering Technology, Benghazi.

## 6. REFERENCES

- Mohanty S, Mohanta GK, Senapati AK, Rath KC. Taguchi grey relational analysis for optimal process parameter of low carbon steel welded by GTAW by using ER309L filler material. *Mater Today: Proc*, 2021;44:2556-2561.  
<https://doi.org/10.1016/j.matpr.2020.12.631>
- Assefa AT, Ahmed GMS, Alamri S, Edacherian A, Jiru MG, Pandey V, et al. Experimental investigation and parametric optimization of the tungsten inert gas welding process parameters of dissimilar metals. *Mater*, 2022;15(13): 4426.  
<https://doi.org/10.3390/ma15134426>.
- Shrivastava M, Kumar R. Optimization of GTA welding parameters for AISI 304 stainless steel using Taguchi method. *Int. Conf. Adv. Res. Innov.* 2020. Available from:  
[https://papers.ssrn.com/sol3/papers.cfm?abstract\\_id=3566687](https://papers.ssrn.com/sol3/papers.cfm?abstract_id=3566687)
- İrsel G. Study of the microstructure and mechanical property relationships of shielded metal arc and TIG welded S235JR steel joints. *Mater Sci Eng A*. 2022; 830:142320.  
<https://doi.org/10.1016/j.msea.2021.142320>
- Dubey Y, Sharma P, Singh MP. Experimental investigation for GTAW optimization using genetic algorithm on S-1 tool steel. *Mater Today: Proc*. 2023.  
<https://doi.org/10.1016/j.matpr.2023.02.174>
- Hariprasath P, Sivaraj P, Balasubramanian V, Pilli S, Sridhar K. Effect of the welding technique on mechanical properties and metallurgical characteristics of the naval grade high strength low alloy steel joints produced by SMAW and GMAW. *CIRP J Manuf Sci Tech*, 2022;37:584-595.  
<https://doi.org/10.1016/j.cirpj.2022.03.007>
- Liu X, Guo Z, Bai D, Yuan C. Study on the mechanical properties and defect detection of low alloy steel weldments for large cruise ships. *Ocean Eng*. 2022; 258:111815.  
<https://doi.org/10.1016/j.oceaneng.2022.111815>
- Zhao D, Bezgans Y, Vdonin N, Radionova L, Glebov L, Bykov V (2023). Metallurgical and mechanical attributes of gas metal arc welded high-strength low-alloy steel. *Int J Adv Manuf Tech*. 2023; 225(3):1305-1323.
- Sakthivel P, Manobbala V, Manikandan T, Salik ZMA, Rajkamal G. Investigation on mechanical properties of dissimilar metals using MIG welding. *Mater Today: Proc*. 2021; 37:531-536.  
<https://doi.org/10.1016/j.matpr.2020.05.488>
- Jiang J, Peng ZY, Ye M, Wang YB, Wang X, Bao W. Thermal effect of welding on mechanical behavior of high-strength steel. *J Mater Civ Eng*. 2021;33(8):04021186.  
[https://doi.org/10.1061/\(ASCE\)MT.1943-5533.000383](https://doi.org/10.1061/(ASCE)MT.1943-5533.000383)
- Yadav AK, Agrawal MK, Saxena KK, Yelamasetti B. Effect of GTAW process parameters on weld characteristics and microstructural studies of dissimilar welded joints of AA5083 and AA6082: optimization technique. *Int J Interact Des Manuf*. 2023;1-10.  
<https://doi.org/10.1007/s12008-023-01230-x>
- Korkmaz E, Meran C. Mechanical properties and microstructure characterization of GTAW of micro-alloyed hot rolled ferritic XPF800 steel. *Eng Sci Tech Int J*. 2021;24(2):503-513.  
<https://doi.org/10.1016/j.jestch.2020.04.006>
- Hamzaçebi C. Taguchi method as a robust design tool. In: Li P, Pereira PAR, Navas H, editors. *Quality control - intelligent manufacturing, robust design and charts*. IntechOpen: London, UK; 2020.  
<https://doi.org/10.5772/intechopen.94908>
- Chauhan V, Kärki T, Varis J. Optimization of compression molding process parameters for NFPC manufacturing using Taguchi design of experiment and mold flow analysis. *Proc*. 2021;9(10):1853.  
<https://doi.org/10.3390/pr9101853>
- Karpagaraj A, Parthiban K, Ponmani S. Optimization techniques used in gas tungsten arc welding process-A review. *Mater Today: Proc*. 2020; 27:2187-2190.  
<https://doi.org/10.1016/j.matpr.2019.09.093>
- Abima CS, Akinlabi SA, Madushele N, Fatoba OS, Akinlabi ET. Experimental investigation of TIG-welded AISI 1008 carbon steel. *IOP Conf Ser: Mater Sci Eng*. 2021;1107(1):012036.  
<https://doi.org/10.1088/1757-899x/1107/1/012036>
- Jawad M, Jahanzaib M, Ali MA, Farooq MU, Mufti NA, Pruncu CI, et al. Revealing the microstructure and mechanical attributes of pre-heated conditions for gas tungsten arc welded AISI 1045 steel joints. *Int J Press Vessels Pip*. 2021; 192:104440.  
<https://doi.org/10.1016/j.ijpvp.2021.104440>
- American Society for Testing and Materials. Standard test methods for tension testing of metallic materials (ASTM E8/E8M-21). *ASTM Int* [Internet];2022. Available from:  
[https://doi.org/10.1520/E0008\\_E0008M-21](https://doi.org/10.1520/E0008_E0008M-21)
- Mariappan M, Parthasarathi NL, Ravindran R, Lenin K, Raja A. Effect of alternating shielding gases in gas metal arc welding of SA515 Gr 70 carbon steel. *Mater Res Express*. 2021;8(9):095601.  
<https://doi.org/10.1088/2053-1591/ac21e9>

20. Murali P, Gopi R. Experimental investigation of tungsten inert gas welding (TIG) using Ar/Ar-CO<sub>2</sub> shielding gas on alloy steels. *Mater Today: Proc.* 2021; 39:812-817.  
<https://doi.org/10.1016/j.matpr.2020.09.776>
21. World Material. EN 1.0038 steel S235JR material equivalent, properties, composition [Internet]. 2024 [Cited 21 Mar 2024]. Available from:  
<https://www.theworldmaterial.com/1-0038-steel-s235jr-material/>
22. Weld Wire. E6010 welding electrode properties [Internet]. 2024 [Cited 21 Mar 2024]. Available online:  
[https://www.weldwire.net/weld\\_products/ww6013/](https://www.weldwire.net/weld_products/ww6013/)
23. Ratiwi YR, Wibowo SS, The effect of electrode and number of passes on hardness and micro structure of shielded metal arc welding. *IOP Conf Ser: Mater Sci Eng.* IOP Publ. 2019; 515(1): 012072.  
<https://doi.org/10.1088/1757-899x/515/1/012072>
24. ISO, Metallic Materials - Conversion of Hardness Table, ISO 18265 [Internet]. 2024 [Cited 21 Mar 2024]. Available online:  
<https://www.iso.org/obp/ui/#iso:std:iso:18265:ed-2:v1:en>
25. Sonar T, Balasubramanian V, Malarvizhi S, Venkateswaran T, Sivakumar D. An overview on welding of Inconel 718 alloy-Effect of welding processes on microstructural evolution and mechanical properties of joints. *Mater Charact.* 2021; 174:110997.  
<https://doi.org/10.1016/j.matchar.2021.110997>
26. Araújo HR, Torres EA, Apolinário LHR, Vicente ADA, da Silva Júnior DC Santos TFDA. Evaluation of mechanical performance and microstructural aspects of AISI 304 stainless steel welded joints produced by controlled short circuit GMAW and GTAW. *Weld World.* 2022;66(12):2443-2459.  
<https://10.1007/s40194-022-01383-5>
27. Elfallah S. Effect of GTAW on the tensile strength and hardness of mild steel. *Annals of "Dunarea de Jos" University of Galati. Fascicle XII, Weld Equip Technol.* 2022;33:95-100.  
<https://doi.org/10.35219/awet.2022.08>
28. Britto JG, John RA, Murugesan G, Prabhakaran R, Jeevahan J Mageshwaran G. Enhancement of mechanical properties of alloy steel by GTAW with different purge/shielding gases. *FME Trans.* 2020;48(1):149-154.  
<https://doi.org/10.5937/fmet2001149B>
29. Kumar A, Pandey S M, Sirohi S, Fydrych D, Pandey C. P92 steel and inconel 617 alloy welds joint produced using ERNiCr-3 filler with GTAW process: Solidification mechanism, microstructure, mechanical properties and residual stresses. *Heliyon.*2023; e18959.  
<https://doi.org/10.1016/j.heliyon.2023.e18959>
30. Kumar A, Mukherjee S, Agrawal S. Optimization of parameters of dissimilar gas tungsten arc welding using grey relational analysis. *Int. J. Veh. Struct. Syst.* 2020;12(2):157-161.  
<https://doi.org/10.4273/ijvss.12.2.09>